DISSERTATION SUMMARY

A – INTRODUCTION TO THE DISSERTATION

1. Rationale and Urgency of the Study

Zirconium (Zr) is an element of high practical value, and its compounds are widely utilized across numerous fields, including engineering ceramics, refractories, electrochemistry, sensors, catalysis, and advanced technologies.

The primary raw material for producing zirconium compounds is zircon ($ZrSiO_4$), a mineral commonly found in coastal placer deposits and typically recovered alongside other heavy minerals. Vietnam possesses abundant zircon resources distributed along various coastal regions, particularly in the Central provinces. One of the major challenges in the deep processing of zircon stems from the inherently stable crystal structure of $ZrSiO_4$. The strong covalent and ionic bonds between Zr and Si within the crystal lattice endow zircon with exceptional thermal and chemical stability, rendering it resistant to decomposition under conventional reaction conditions. Consequently, breaking down the $ZrSiO_4$ structure to convert zirconium into a leachable and purifiable form represents the key step determining the overall efficiency of zircon processing. In this context, the sub-molten salt (SMS) method utilizing highly concentrated alkaline solutions offers a promising approach.

Beyond the primary goal of synthesizing high-purity ZrO_2, expanding the utilization of zirconium-containing intermediates—such as zirconium oxychloride ($ZrOCl_2$, denoted as ZOC) obtained from concentrate processing—to synthesize value-added materials holds significant practical importance. In this dissertation, ZOC is employed as a zirconium precursor to synthesize an Mg–Zr composite catalyst. The resulting material is characterized and preliminarily evaluated for its catalytic activity in the ethanolysis reaction, thereby exploring the feasibility of utilizing intermediate products from zircon processing for catalytic applications and biofuel production.

2. Research Objectives

+ To investigate the decomposition of Vietnamese zircon concentrate using KOHvia the sub-molten salt (SMS) method and determine the effects of technological parameters on zircon decomposition efficiency.

+ To study the leaching, separation, and purification processes of the post-decomposition products, establishing optimal conditions for synthesizing zirconium oxychloride (ZOC) and preparing high-purity ZrO_2.

+ To synthesize Mg–Zr catalytic materials using ZOC derived from Vietnamese zircon concentrate as the zirconium precursor, and preliminarily evaluate the catalytic performance of the synthesized material.

3. Novel Contributions of the Dissertation

- Characterization and SMS Decomposition: The chemical composition, mineralogical composition, and phase structure of several commercial Vietnamese zircon concentrates were systematically elucidated, establishing a scientific basis for selecting and optimizing a deep-processing route tailored to domestic raw materials. Optimal technological conditions were established for decomposing zircon concentrate with KOH via the sub-molten salt (SMS) method, achieving a $ZrSiO_4$ decomposition efficiency of 99.08%.

- Integrated Deep-Processing Technology Chain: A complete technological chain for the deep processing of zircon concentrate via KOH-SMS—integrating leaching, recovery, and purification of intermediate zirconium compounds—was developed to produce ZrO_2 with a purity reaching 99.57%. This represents a valuable scientific and technological achievement toward the deep processing of zircon in Vietnam.

- Value-Added Catalytic Application: The zirconium precursor recovered from Vietnamese zircon concentrate was successfully utilized to synthesize an Mg–Zr catalyst and evaluated for converting high-free-fatty-acid lipid feedstocks into biodiesel. Experimental results demonstrated the production of biodiesel with a fatty acid ethyl ester (FAEE) content exceeding 94% under the investigated conditions. These findings preliminarily demonstrate the feasibility of linking deep mineral processing with the development of value-added

zirconium products, opening a pathway from domestic mineral resources to ZrO_2-based functional materials.

4. Structure of the Dissertation

The dissertation comprises 114 pages (excluding appendices and references) and is organized into the following sections: Introduction (2 pages), Chapter 1: Literature Review (38 pages), Chapter 2: Experimental and Methodology (19 pages), Chapter 3: Results and Discussion (54 pages), and Conclusions (2 pages). The dissertation contains 33 tables, 44 figures and graphs, and 112 references.

B – MAIN CONTENT OF THE DISSERTATION

CHAPTER 1 – LITERATURE REVIEW

In this chapter, the author provides a comprehensive review of zircon ores and Vietnamese zircon concentrates; zircon concentrate processing technologies, with particular emphasis on the sub-molten salt (SMS) method; synthesis methods for ZrO_2 materials; and the application of zirconium-based precursors in the preparation of Mg–Zr catalysts.

CHAPTER 2 – EXPERIMENTAL AND RESEARCH METHODOLOGY

All experiments were conducted at the National Key Laboratory for Petrochemical and Refinery Technologies, Vietnam Institute of Industrial Chemistry (VIIC).

2.1. Processing of Zircon Concentrate

2.1.1. Decomposition of Zircon Concentrate by Alkaline Agent via the Sub-Molten Salt (SMS) Method

The decomposition of zircon concentrate via the sub-molten salt method in an alkaline medium was carried out in a stainless-steel autoclave reactor equipped with automated heating control, mechanical agitation, and an internal cooling coil.

2.1.2. Leaching of Post-Decomposition Concentrate to Produce Intermediate ZOC

a. Treatment of SMS Decomposition Products: Upon completion of the SMS reaction, the reaction mixture was cooled to 80–90 °C, and an appropriate amount of deionized water was added under continuous stirring to completely dissolve excess KOH and water-soluble K_2SiO_3. The slurry was separated by vacuum filtration, and the filter cake was washed once more with deionized water. The filtrate was collected for concentration and crystallization to recover K_2SiO_3 and recycle KOH.

b. Recovery of K_2SiO_3 and Treatment of KOH for reuse: The filtrate obtained from treating the SMS decomposition product, containing predominantly dissolved K_2SiO_3 and excess KOH, was concentrated using a rotary vacuum evaporator or circulating evaporator until saturation was reached. Subsequently, the solution was slowly cooled to room temperature to induce the crystallization of $K_2SiO_3 \cdot xH_2O$. The remaining mother liquor containing KOH can be recycled for subsequent reaction cycles.

c. Acid Leaching with HCl: The filter cake obtained from the water-washing stage (containing the primary zirconium reaction products) was leached with HCl solutions of varying concentrations. Vacuum filtration was then performed to separate insoluble solid residues (impurities) from the liquid phase, while the decomposed zirconium phases dissolved completely in HCl to form an acid leach liquor.

d. Removal of Residual Silicon Impurities: A flocculating agent (polyethylene glycol, PEG) was added to the HCl leach liquor to remove residual dissolved silica (SiO_2) via coagulation–flocculation. Following sedimentation and vacuum filtration, the precipitated SiO_2 gel was separated, yielding a clarified filtrate containing excess HCl and dissolved $ZrOCl_2$.

e. Recovery of Crystalline $ZrOCl_2$: The clarified leach solution was concentrated in a 1 L rotary vacuum evaporator and subsequently cooled to crystallize $ZrOCl_2 \cdot 8H_2O$. The crystals were dried at 70 °C for 12–15 hours to obtain the crude $ZrOCl_2 \cdot 8H_2O$(ZOC) product.

2.1.3. Purification of $ZrOCl_2$

Because the purity of the first-crystallization ZOC is insufficient for high-grade applications, further purification is required to enhance the purity of this intermediate and ultimately obtain high-purity ZrO_2.

2.1.4. Conversion of ZOC to ZOH and Thermal Treatment of ZOH to Produce ZrO_2

Conversion of crystalline ZOC into intermediate zirconium oxyhydroxide (ZOH)

Step 1: Second-crystallization ZOC crystals were dissolved in distilled water at a specified liquid-to-solid ratio and stirred at 150 rpm for approximately 15 minutesat room temperature.

Step 2: The stirring speed was reduced to 50 rpm, and a predetermined volume of 10% NH_4OH solution was added dropwise to the solution from Step 1 until precipitation reached equilibrium.

Step 3: Solid–liquid separation was performed by filtration.

Thermal treatment of ZOH to produce ZrO_2:

Step 4: The solid cake from Step 3 was dispersed in water to form a suspension of a defined concentration and spray-dried to obtain ZOH powder. The intermediate ZOH powder was then calcined under specified temperature and time conditions.

Step 5: After calcination, the product was cooled to room temperature and finely milled.

2.2. Synthesis and Preliminary Catalytic Activity Evaluation of Mg–Zr Catalyst from Zirconium Precursor Derived from Vietnamese Zircon Concentrate

2.2.1. Catalyst Synthesis

- $MgCl_2 \cdot 6H_2O$ and purified $ZrOCl_2 \cdot 8H_2O$ were dried at 70 °C for 12 hours to remove surface moisture.

- $MgCl_2.6H_2O$ and $ZrOCl_2 \cdot 8H_2O$ corresponding to a molar ratio of Mg : Zr = 1: 1 were dissolved in deionized water and mixed under continuous stirring at room temperature. 1 M NH_4OH solution was slowly added dropwise

until the pH reached approximately 10 to co-precipitate the Mg–Zr hydroxide mixture. The resulting suspension was aged for 12 hours, filtered, and washed repeatedly with deionized water until no Cl^- ions were detected in the wash water using an $AgNO_3$ test. The washed precipitate was dried overnight at 110 °C to obtain the Mg–Zr precursor.

- The dried precursor was calcined in air at temperatures of 500, 600, 800, and 1000 °C. The calcined samples were stored in a desiccator prior to physicochemical characterization and catalytic activity testing.

2.2.2. Catalytic Activity Evaluation

The catalytic activity was preliminarily evaluated via the ethanolysis of refined coconut oil. The reaction was conducted in a stainless-steel batch reactor using ethanol as the reactant, with an ethanol-to-oil molar ratio of 40: 1, a catalyst loading of 10 wt% relative to the oil feedstock, a stirring speed of 600 rpm, and a reaction time of 2 hours.

Following the reaction, the catalyst was separated, and the liquid product was treated and analyzed to determine the content of fatty acid ethyl esters (FAEE) by gas chromatography–mass spectrometry (GC–MS, Agilent 7890B-5977A equipped with an HP-5 MS capillary column, 30 m × 0.25 mm × 0.25 μm).

2.3. Physicochemical Characterization and Product Analysis Methods

Raw materials, intermediates, final products, and catalysts were characterized using modern analytical techniques, including X-ray diffraction (XRD), thermogravimetric analysis (TGA/TG-DTA), gas chromatography–mass spectrometry (GC–MS), X-ray fluorescence (XRF), scanning electron microscopy (SEM), laser diffraction particle size analysis, and wet chemical analysis.

CHAPTER 3 – RESULTS AND DISCUSSION

3.1. Collection and Technical Specifications of Commercial Zircon Concentrate Samples in Vietnam

Information regarding the commercial zircon concentrate samples collected from the Vietnamese market is presented in **Table 3.1.**

Table 3.1. Information and technical specifications of commercial zircon concentrate samples in Vietnam

No.	Sample Code	Published Specifications and Origin
1	TVU-Zr-000	Origin: Grade 1 Zircon Concentrate, produced by Hung Thinh Titanium Slag One Member Co., Ltd., mined from the Binh Thuan deposit cluster. Chemical composition: Total $ZrO_2 + HfO_2 \geq 65\%$; $SiO_2 \leq 32\%$; $TiO_2 \leq 0.2\%$; $Al_2O_3 \leq 0.50\%$; $Fe_2O_3 \leq 0.15\%$; $P_2O_5 \leq 0.15\%$; $U + Th \leq 0.01\%$. Particle size: Average 125 μm.
2	Zr-HTN-BT	Origin: Zircon concentrate mined from the Ham Thuan Nam deposit cluster, Binh Thuan province. Technical specifications: No updated commercial sheet available (due to the suspension of the titanium mining project following the 2022 landslide incident, the associated zircon concentrate is no longer mined or commercially traded).
3	Zr-BĐ	Chemical composition: $ZrO_2 \geq 65\%$; $Fe_2O_3 \leq 0.1\%$; $TiO_2 \leq 0.3\%$. Particle size: ≤ 45 μm.

Table 3.2. Mineralogical composition of commercial zircon concentrate samples

No	Sample Code	Mineralogical composition %			
		$ZrSiO_4$	K_2ZrSiO_4	$K_2Zr_2O_5$	SiO_2
1	TVU-Zr-000	93 - 95	-	-	2 - 4
2	Zr-HTN-BT	94 - 96	-	≤ 1	1 - 3
3	Zr-BĐ	92 - 94	-	-	3 - 5

The analytical results in **Table 3.2** indicate that all commercial concentrate samples contain a high zircon ($ZrSiO_4$) content (> 92%) and low impurity levels. However, whereas the impurities in samples TVU-Zr-000 and Zr-BĐ consist almost exclusively of free SiO_2 (2–4% and 3–5%, respectively), sample Zr-HTN-BT also contains a minor amount of $K_2Zr_2O_5$ (≤ 1%).

Table 3.3. Chemical composition of the zircon concentrate samples (determined by XRF)

TT	Parameters	Chemical composition, %		
		TVU-Zr-000	**Zr-HTN-BT**	**Zr-BĐ**
1	MKN (LOI)	0.23	0.55	0.31
2	ZrO_2	73.60	66.9	66.1
3	SiO_2	19.50	24.2	25.1
4	HfO_2	3.82	5.41	4.82
5	Al_2O_3	0.87	1.04	0.324
6	Na_2O	0.75	0.402	0.340
7	Y_2O_3	0.26	0.218	0.212
8	SO_3	0.0975	0.179	0.215
9	TiO_2	0.19	0.417	1.84
10	CaO	0.15	0.161	0.0819
11	Fe_2O_3	0.15	0.102	0.151
12	WO_3	0.11	0.0672	0.174
13	U_3O_8	0.0792	0.0926	0.108
14	Nb_2O_5	0.0581	0.0637	0.0679
15	P_2O_5	0.0424	0.21	0.13
16	ThO_2	0.0268	0.0370	-
17	Cr_2O_3	0.0132	-	-
18	MnO	0.0112	0.0130	0.0089
19	MgO	-	-	0.0332
20	Bi_2O_3	-	-	0.0255
21	V_2O_5	-	-	0.0182

TT	Parameters	Chemical composition, %		
		TVU-Zr-000	Zr-HTN-BT	Zr-BĐ
22	K_2O	-	0.0471	0.0347

3.2. Decomposition of Zircon Concentrate via the Sub-Molten Salt (SMS) Process

3.2.1. Selection of Alkaline Agent for SMS Decomposition of Binh Thuan Zircon Concentrate

The concentrate decomposition efficiencies of two alkaline agents, NaOHand KOH, were compared, and the results are shown in **Figure 3.1**.

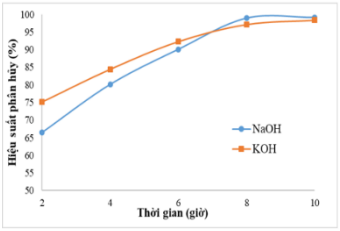

Figure 3.1. SMS decomposition reaction using KOH and NaOH agents

The results demonstrate that the SMS process (under identical conditions) achieves very high zircon decomposition efficiencies with both alkaline agents. After 8 hours of reaction, the decomposition efficiency reached approximately 98.93% for NaOH and 97.12% for KOH. Although the 8-hour efficiency of KOH is slightly lower than that of NaOH, KOH exhibits a significantly faster initial reaction rate. Employing KOH at elevated temperatures accelerates the breakdown of zircon compared to NaOH because the lower viscosity of the KOH sub-molten medium enhances mass transfer. Therefore, when other reaction parameters are comparable, reaching the decomposition plateau earlier makes KOH a more promising reagent than NaOH. Furthermore, when KOH is used, the reaction by-product (K_2SiO_3) can be utilized as a potassium-silicate fertilizer, thereby reducing waste treatment costs and generating a valuable co-product. Consequently, KOH was selected as the alkaline agent for decomposing zircon concentrate via the SMS method.

3.2.2. Investigation of Technological Parameters Affecting Zircon Concentrate Decomposition via the SMS Method

3.2.2.1. Effect of Initial KOH Concentration

To establish a sub-molten salt reaction medium, a highly concentrated KOH solution is required. Therefore, initial KOH concentrations starting from 50 wt% were investigated, as summarized in **Table 3.4**.

Table 3.4. Effect of initial KOH concentration on concentrate decomposition efficiency

TT	KOH concentration, % wt	Decomposition efficiency, %
1	50	69.38
2	60	78.51
3	70	89.72
4	80	97.12
5	85	97.15

An initial KOH concentration of 80 wt% was selected for subsequent experiments to ensure high decomposition efficiency while maintaining process economics.

3.2.2.2. Effect of Reaction Temperature

The effect of reaction temperature was investigated over the range of 200–300 °C, and the results are presented in **Figure 3.2**.

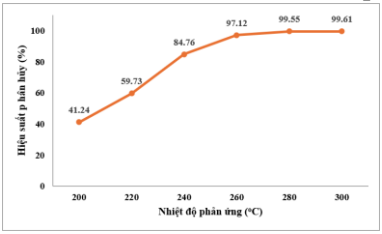

Figure 3.2. Zircon concentrate decomposition efficiency at different temperatures

A temperature of 280 °C was determined to be optimal for decomposing zircon concentrate with 80 wt% KOH over an 8-hour reaction period.

3.2.2.3. Effect of KOH/$ZrSiO_4$ Molar Ratio

As shown in **Figure 3.3**, a decomposition efficiency exceeding 99% was achieved at a KOH/$ZrSiO_4$ molar ratio of 4.8: 1, which was selected as the optimal ratio for the SMS decomposition of zircon.

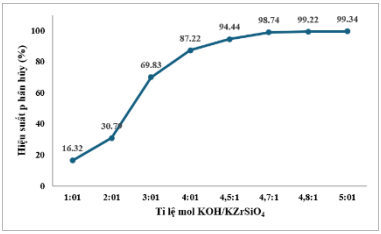

Figure 3.3. Effect of* KOH/ $ZrSiO_4$ *molar ratio on concentrate decomposition efficiency

3.2.2.4. Effect of Stirring Speed

A stirring speed of 250 rpm was found to be suitable and was selected for subsequent studies (**Figure 3.4**).

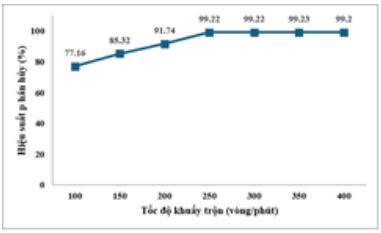

Figure 3.4. Effect of stirring speed on concentrate decomposition efficiency

3.2.2.5. Effect of Reaction Time

The effect of reaction time is illustrated in **Figure 3.5**. A reaction time of 6 hours was found to be optimal, ensuring a high decomposition efficiency (99.08%) while avoiding prolonged heating that would waste energy and reduce the economic viability of the process.

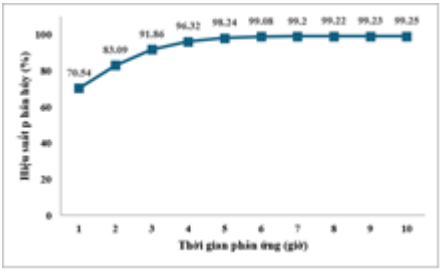

Figure 3.5. Effect of reaction time on concentrate decomposition efficiency

3.3. Leaching of Post-Decomposition Products to Synthesize Intermediate $ZrOCl_2$

3.3.1. Leaching of SMS Decomposition Products Using HCl

Following the SMS decomposition of zircon with KOH and water washing, the resulting solid phase (obtained as a thick slurry) was treated with HCl solution to dissolve zirconium into the aqueous phase as $ZrOCl_2$.

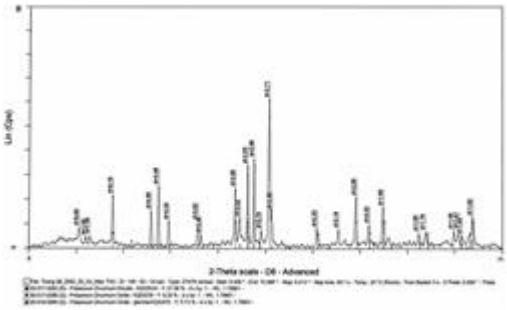

Figure 3.6. XRD pattern of the solid product after SMS decomposition of zircon concentrate

The XRD pattern of the post-SMS decomposition product (**Figure 3.6**) reveals the presence of K_2ZrSiO_4, characterized by diffraction peaks at $2\theta = 17°$, 36°, and 38°(corresponding to $d = 6.17$, 2.86, and 2.71 AA), and $K_2Zr_2O_5$at $2\theta = 37°$ and $54°$(corresponding to $d = 2.93$ and 1.96 AA). The absence of characteristic $ZrSiO_4$ peaks confirms complete decomposition with negligible unreacted zircon remaining.

3.3.1.1. Effect of HCl Concentration

Table 3.5. Effect of HCl concentration on product leaching efficiency

TT	HCl concentration, % wt	Leaching efficiency ,%
1	36,5	63.61
2	30	78.73
3	25	99.55
4	20	99.55
5	15	99.56
6	10	99.56

TT	HCl concentration, % wt	Leaching efficiency ,%
7	5	83.62

3.3.1.2. Effect of Leaching Temperature

Table 3.6. Effect of reaction temperature on leaching efficiency using 10% HCl

STT	Temperature, ^{o}C	Leaching efficiency ,%
1	25	99.56
2	30	99.53
3	35	99.50
4	40	99.44
5	45	99.41
6	50	99.43
7	55	98.46
8	60	98.31

Ambient temperature (25 ˚C) is sufficient for complete reaction and offers greater technological convenience.

3.3.1.3. Effect of HCl-to-Material Ratio

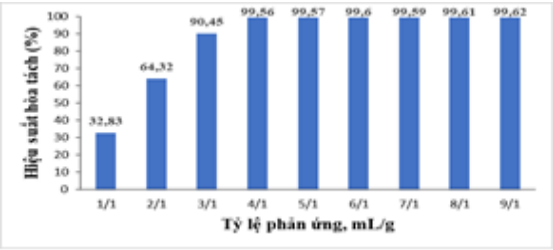

Figure 3.7. Effect of reactant ratio on leaching efficiency

Based on the experimental results shown in **Figure 3.7**, a liquid-to-solid ratio of 4: 1 (mL/g)was selected.

3.3.1.4. Effect of Reaction Time

The results presented in **Figure 3.8** indicate that a reaction time of 5 minutesis sufficient for complete leaching.

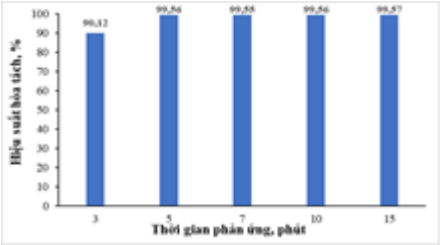

***Figure 3.8. Effect of time on leaching efficiency with* 10% HCl**

3.3.1.5. Effect of Stirring Speed

Based on the results in **Table 3.7**, a stirring speed of 250 rpm was selected for subsequent experiments.

Table 3.7. Effect of stirring speed on leaching efficiency (5-minute reaction time)

No.	Stirring Speed (rpm)	Leaching Efficiency (%)
1	50	57.82
2	100	73.21
3	150	89.65
4	200	93.47
5	250	97.85
6	300	98.20

3.3.2. Removal of Silicon-Containing Compounds via Coagulation–Flocculation

After HCl leaching, the intermediate solution primarily contains zirconium ions along with a small amount of dissolved silicon. Therefore, a gelation–flocculation step is required to remove silicon prior to $ZrOCl_2$ purification. The selected purification approach combines HCl acid treatment with polyethylene glycol (PEG)-assisted gelation and flocculation.

3.3.2.1. Effect of HCl Concentration

Following solid–liquid separation, the leach liquor underwent gelation in an acidic medium with the addition of 25 wt% PEG flocculant under the

following conditions: HCl concentration of 10–25 wt%, $V_{\text{HCl solution}}/m_{\text{material}} = 4{:}1$ mL/g, temperature of 100 °C, and reaction time of 30 minutes. After gelation and cooling to room temperature, the silica gel was separated from the solution by vacuum filtration.

Table 3.8. Effect of acid concentration on silicon removal

No.	HCl Concentration (wt%)	Si Removal Efficiency (%)	Observation
1	10	81.15	Colloidal suspension, difficult to filter
2	15	87.21	Colloidal suspension, difficult to filter
3	20	98.83	Slow settling, difficult to filter
4	25	99.26	Rapid settling, easy to filter

The experimental results in **Table 3.8** demonstrate that at an HCl concentration of 25 wt%, silicon is almost completely removed (99.26%), and the resulting gel settles rapidly, facilitating easy filtration.

3.3.2.2. Effect of Gelation Temperature

Table 3.9. Effect of temperature on the gelation process

No.	Temperature (°C)	Si Removal Efficiency (%)
1	80	80.62
2	90	86.24
3	100	99.26
4	110	99.28

The results in **Table 3.9** indicate that 100 °C is the most suitable temperature for the gelation process.

3.3.2.3. Effect of Gelation Time

As shown in **Table 3.10**, gelation is virtually complete after 30 minutes, and extending the time further yields no significant improvement.

Table 3.10. Effect of time on the gelation process

No.	Time (minutes)	Si Removal Efficiency (%)
1	15	83.64
2	20	88.29
3	30	99.26
4	40	99.31

3.3.2.4. Effect of Acid-to-Material Ratio

Experimental results are presented in **Table 3.11**. Efficiency exceeds 99% starting from a ratio of 2: 1 (mL/g) (expressed as 1: 2 g/mL in table notation), indicating that a 2 mL/gratio is technically and economically superior to 4 mL/g.

Table 3.11. Effect of **25%** *HCl-to-material ratio on leaching efficiency*

STT	Ratio of Material to 25% HCl ($m_{material}/V_{HCl}$, g/mL)	Leaching Efficiency (%)
1	1:1	82.51
2	1:2	99.55
3	1:3	99.55
4	1:4	99.26

3.3.3. Concentration and Crystallization of $ZrOCl_2$

After removing the PEG–Si gel, the solution mainly contains dissolved $ZrOCl_2$ (ZOC) along with minor iron impurities. To recover pure ZOC crystals, the solution was concentrated, aged, and crystallized—a critical step in converting zircon concentrate into high-quality ZrO_2.

3.3.3.1. Effect of Equivalent ZrO_2Concentration in Solution on Crystallization Efficiency

The results are presented in **Table 3.12**, showing that the solution should be concentrated to approximately 16% of its initial volume.

Table 3.12. Effect of concentration degree on equivalent ZrO_2 concentration and ZOC crystallization efficiency

No.	Solution Volume After Concentration (% of initial volume)	Equivalent ZrO_2 Concentration (g/mL)	Crystallization Efficiency (%)
1	90	0.116	0.0
2	70	0.149	0.0
3	25	0.416	26.6
4	20	0.520	30.4
5	18	0.578	34.9
6	16	0.646	62.8
7	14	0.743	63.0
8	10	1.040	63.1

3.3.3.2. Effect of Aging Time

Experimental results on the effect of aging time on first-stage ZOC crystallization recovery (**Table 3.13**) indicate that an aging time of 60 minutesis optimal.

Table 3.13. Dependence of first-stage crystallization efficiency on aging time

Aging Time (minutes)	Cumulative First-Stage Crystallization Efficiency (%)
0 (immediately after cooling)	0.0
10	18.1
20	34.6
30	46.0
45	60.0
60	62.8
90	63.0

3.3.3.3. Washing and Purification of ZOC Crystals Obtained from Concentration–Crystallization

Table 3.14. Main chemical composition of ZOC before and after HCl washing

No.	Chemical Component	Concentration, % wt	
		Before HCl Washing (wt%)	After HCl Washing (wt%)
1	ZrO_2	37.372	37.496
2	HfO_2	0.783	0.796
3	Nd_2O_3	0.078	0.069
4	Cs_2O	0.138	0.121
5	As_2O_3	0.132	0.112
6	ZnO	0.004	0.004
7	Fe_2O_3	0.023	0.021
8	Cr_2O_3	0.010	0.008
9	Cl	17.702	17.502
10	SiO_2	0.042	0.032
11	Al_2O_3	0.022	0.016

Table 3.15. Chemical composition of ZrO_2 (obtained by direct calcination of ZOC)

No.	Chemical Component	Hàm lượng (% khối lượng)	
		Before HCl Washing (wt%)	After HCl Washing (wt%)
1	ZrO_2	97.027	97.036
2	HfO_2	1.502	1.533
3	SiO_2	0.1767	0.1754
4	Fe_2O_3	0.0396	0.038
5	SO_3	0.4851	0.4837

No.	Chemical Component	Hàm lượng (% khối lượng)	
		Before HCl Washing (wt%)	After HCl Washing (wt%)
6	CaO	0.0725	0.0719
7	NiO	0.0285	0.0275
8	Y_2O_3	0.541	0.53
9	Nd_2O_3	0.2356	0.2335
10	Bi_2O_3	0.7874	0.7832
11	PbO	0.1337	0.1318
12	Al_2O_3	0.0972	0.0968

The data in both **Table 3.14** and **Table 3.15** indicate that the compositional difference before and after HCl washing is negligible, demonstrating that the ZOC crystals formed during crystallization already possess a relatively high degree of purity.

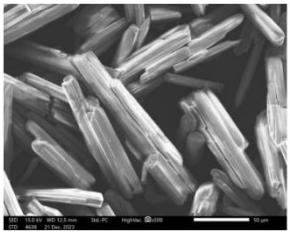

Figure 3.9. SEM micrograph of the $\mathbf{ZrOCl_2 \cdot 8H_2O}$ ***sample***

The SEM micrograph of the $ZrOCl_2 \cdot 8H_2O$sample (**Figure 3.9**) reveals well-defined needle-like (acicular) crystals with uniform morphology and size, confirming a well-controlled crystallization process. The synthesized ZOC exhibits a combined $(ZrO_2 + HfO_2)$ content of 38.155 wt% (before washing) to 38.292 wt% (after washing), which is in close agreement with literature values (38.39%, ref. [106]), confirming that the ZOC synthesis parameters were appropriate. Furthermore, the number of impurity elements decreased substantially compared to the

initial zircon concentrate (from 17 down to 10 impurity components), demonstrating effective purification.

3.4. Purification of $ZrOCl_2$

3.4.1. Conversion of ZOC into Zirconium Basic Sulfate (ZBS) Precipitate

The precipitation of zirconium basic sulfate (ZBS) was carried out by adding $(NH_4)_2SO_4$ according to the following chemical equation:

$$5ZrOCl_2.8H_2O + 2(NH_4)_2SO_4 \rightarrow Zr_5O_8(SO_4)_2.15H_2O + 4NH_4Cl + 6HCl + 22H_2O$$

3.4.1.1. Effect of Reaction Medium pH on ZBS Precipitation Efficiency

As shown in **Table 3.16**, pH = 7 was selected for subsequent studies to ensure high precipitation efficiency, good selectivity, and minimal impurity co-precipitation.

Table 3.16. Effect of pH on ZBS precipitation efficiency

No.	pH	Precipitation Efficiency (%)
1	3	-
2	4	32.47
3	5	63.59
4	6	97.14
5	7	99.35
6	8	99.37

3.4.1.2. Effect of Temperature on ZBS Formation Efficiency

The results presented in **Figure 3.10** indicate that 25 °C is the optimal temperature, ensuring high yield while avoiding unnecessary energy consumption.

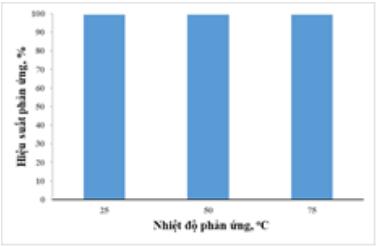

Figure 3.10. Effect of reaction temperature on ZBS precipitation efficiency

3.4.1.3. Effect of Reaction Time on the Conversion of ZOC to ZBS

Table 3.17 shows that the reaction proceeds rapidly; a reaction time of 15 minutesis optimal for achieving near-complete conversion.

Table 3.17. Effect of reaction time on ZBS precipitation efficiency

No.	Time (minutes)	Precipitation Efficiency (%)
1	5	48.82
2	10	67.39
3	15	99.35
4	20	99.36
5	25	99.35
6	30	99.35

3.4.2. Conversion of ZBS into Zirconium Oxyhydroxide (ZOH)

The phase conversion of ZBS precipitate into $ZrO(OH)_2(ZOH)$ using NH_4OHproceeds according to the following reaction:

$$5ZrOCl_2.8H_2O + 2(NH_4)_2SO_4 \rightarrow Zr_5O_8(SO_4)_2.15H_2O + 4NH_4Cl + 6HCl + 22H_2O$$

3.4.2.1. Effect of Reaction Medium pH on ZOH Conversion Efficiency

Table 3.18. Effect of pH on ZOH precipitation conversion efficiency

TT	Solution pH	Conversion Efficiency (%)
1	7,5	30.89
2	8	41.93
3	8,5	67.19
4	9	79.33

TT	Solution pH	Conversion Efficiency (%)
5	9,5	97.78
6	10	99.25
7	10,5	99.26
8	11	99.26

The results in **Table 3.18** demonstrate that $pH = 10$ is suitable for achieving complete conversion of ZBS into ZOH.

3.4.2.2.Effect of Temperature on ZBS-to-ZOH Conversion Efficiency

Table 3.19. Effect of temperature on ZBS-to-ZOH conversion efficiency

No.	Temperature (˚C)	Conversion Efficiency (%)
1	25	76.74
2	40	86.42
3	50	91.36
4	60	98.44
5	70	99.25
6	80	99.26

As shown in **Table 3.19**, the conversion efficiency reaches a maximum of 99.25% at 70 ˚C and remains virtually unchanged when the temperature is raised to 80 ˚C. Consequently, 70 ˚C was identified as the optimal temperature for subsequent experiments.

3.4.2.3. Effect of Reaction Time

Table 3.20. Effect of reaction time on ZBS-to-ZOH conversion efficiency

No.	Time (minutes)	Conversion Efficiency (%)
1	15	46.69
2	30	85.68
3	45	99.25
4	60	99.26
5	70	99.27

The optimal reaction time was selected as 45 minutes.

After obtaining ZOH, purification was continued by re-dissolving ZOH in HCl to form ZOC, followed by concentration and a second crystallization to obtain high-purity ZOC. The purified ZOC was then converted into high-purity ZOH. Based on the TG–DTA thermogram (**Figure 3.11**), thermal treatment of ZOH was carried out to produce pure ZrO_2.

Based on the XRD patterns (**Figure 3.12**), calcination at 900 °C for 70 minuteswas selected as the optimal thermal treatment condition to obtain thermally stable monoclinic ZrO_2.

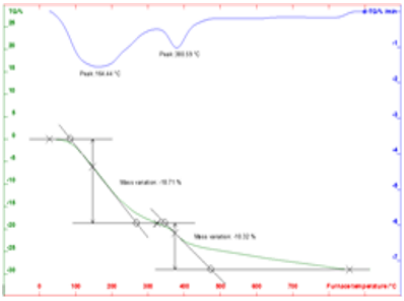

Figure 3.11. TG–DTA curves of the intermediate ZOH sample

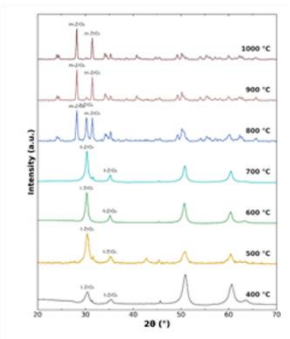

Figure 3.12. XRD patterns of ZrO_2 calcined at different temperatures

3.5. Characterization of ZrO_2 Synthesized from Vietnamese Zircon Concentrate

The synthesized ZrO_2 product was comprehensively analyzed and evaluated using multiple physicochemical techniques. Its chemical composition is summarized in **Table 3.21**, revealing high purity with a combined $ZrO_2 + HfO_2$ content of 99.57%. This result is consistent with the XRD pattern of the final product (**Figure 3.13**), which exhibits sharp diffraction peaks and a low baseline, indicative of high crystallinity. Two

prominent reflections at $2\theta \approx 28.2°$and 31.5°, along with secondary peaks, confirm the presence of the monoclinic zirconia phase (m-ZrO_2).

Table 3.21. Chemical composition of the synthesized ZrO_2product

No.	Component	Content	Unit
1	ZrO_2	99.270	%
2	HfO_2	0.301	%
3	SiO_2	542	ppm
4	SO_3	284	
5	CaO	316	
6	Fe_2O_3	99	
7	NiO	47	
8	Y_2O_3	115	
9	Nd_2O_3	334	
10	Bi_2O_3	88	
11	PbO	119	
12	Al_2O_3	279	

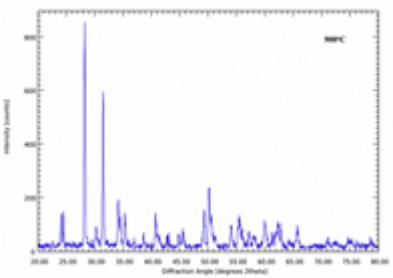

Figure 3.13. XRD pattern of the obtained ZrO_2product

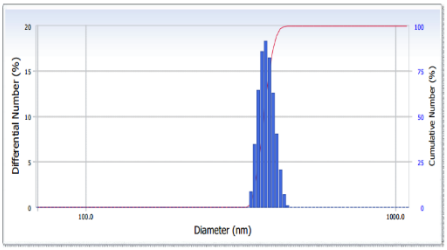

Figure 3.14. Number-based particle size distribution of the ZrO_2sample

Particle size distribution analysis via laser diffraction (**Figure 3.14**) demonstrates that the majority of ZrO_2 particles fall within the range of 0.34 –0.45 μm, with an average particle size of 0.38 μm.

3.6. Preliminary Evaluation of the Catalyst Synthesized from Vietnamese Zircon Concentrate

The precursors employed in this study were analytical-grade $MgCl_2 \cdot 6H_2O$and purified $ZrOCl_2 \cdot 8H_2O$ derived from the Vietnamese zircon concentrate purification process.

The XRD pattern of the catalyst calcined at 1000 ˚C for 2 hours (ZM-1000-2h), presented in **Figure 3.16**, shows characteristic peaks corresponding to monoclinic ZrO_2(M) and MgO integrated within a perovskite-type composite structure, confirming the successful synthesis of the Mg–Zr composite oxide catalyst.

The SEM micrograph of the ZM-1000-2h catalyst sample (**Figure 3.15**) reveals dense, spherical or rounded polyhedral particles with smooth facets (~ 200–500 nm). The particles aggregate into clusters and exhibit necking/sintering at contact points, reflecting the ceramic nature of the calcined catalytic material.

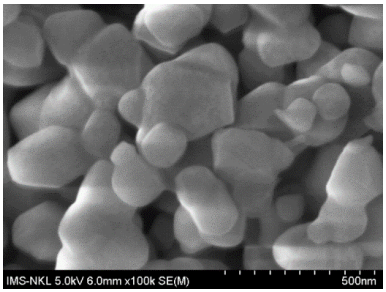

Figure 3.15. SEM micrograph of the ZM-1000-2h catalyst

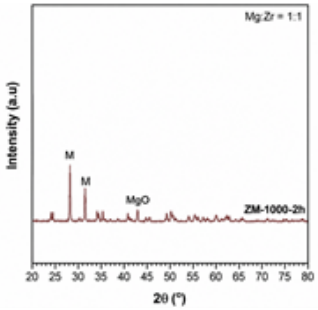

Figure 3.16. XRD pattern of the Mg–Zr mixed oxide calcined at **1000 ˚*C***

To preliminarily evaluate the applicability of the catalyst in biodiesel synthesis, the catalytic activity of ZM-1000-2h was tested in the ethanolysis of refined coconut oil (acid value < 0.1 mg KOH $\cdot$ g^{-1}). Within the scope of this dissertation, this test serves as an application-oriented proof-of-concept and preliminary activity assessment; in-depth investigations into the morphology, physicochemical properties, and catalytic performance across diverse lipid feedstocks will be conducted in future work.

The GC–MS analysis results of the ethanolysis product are displayed in **Figure 3.17** and summarized in **Table 3.22**.

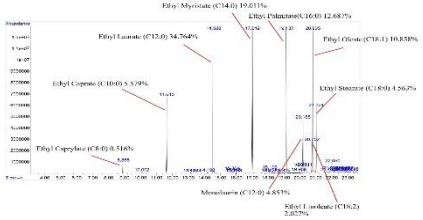

Figure 3.17. GC–MS chromatogram of the product obtained from the ethanolysis of refined coconut oil

Table 3.22. Product distribution by GC–MS for the ethanolysis of refined coconut oil

Component	**Diện tích pic (%)**
Ethyl Caprylate (C8:0)	0.516
Ethyl Caprate (C10:0)	5.579
Ethyl Laurate (C12:0)	34.764
Ethyl Myristate (C14:0)	19.011
Ethyl Palmitate (C16:0)	12.67
Glycerol Monolaurate	4.853
Glycerol Myristate	–
Ethyl Oleate (C18:1)	10.858
Ethyl Stearate (C18:0)	4.563
Ethyl Linoleate (C18:2)	2.027
Total Peak Area of Esters (%)	94.85
Total Peak Area of Non-Esters (%)	5.15

The data in **Table 3.22** confirm the predominant formation of medium-chain fatty acid ethyl esters (C12–C16), which are characteristic of coconut oil. The ZM-1000-2h catalyst exhibited high total ester selectivity 94.85% and a very low non-ester residue 5.15%, reflecting the well-developed ceramic structure of ZM-1000-2h. By comparison, a blank control experiment conducted under identical reaction conditions without a catalyst yielded a conversion of less than 5%, confirming the high catalytic activity of ZM-1000-2h.

CONCLUSIONS

1. The dissertation comprehensively investigated and systematically evaluated the chemical composition, mineralogical composition, and phase structure of commercial zircon concentrates from Binh Thuan and Binh Dinh, Vietnam. The results demonstrate that the primary zirconium-bearing mineral phase in the concentrates is $ZrSiO_4$(exceeding 90 wt%), accompanied by valuable transition metals and heavy rare earth elements such as Hafnium (Hf), Yttrium (Y), and Niobium (Nb). These baseline data provide a critical foundation for designing a deep-processing route to maximize Zr recovery at minimal cost, ensuring the efficient utilization of Vietnam's zircon resources.

2. Optimal technological conditions were established for decomposing zircon concentrate via the sub-molten salt (SMS) method using KOH, which provides lower melt viscosity, faster decomposition kinetics, and shorter reaction times compared to NaOH: initial KOHconcentration of 80 wt%, reaction temperature of 280 °C, KOH/$ZrSiO_4$molar ratio of 4.8: 1, reaction time of 6 hours, and stirring speed of 250 rpm. Under these conditions, the $ZrSiO_4$ decomposition efficiency reached 99.08%.

3. The acid leaching and zirconium recovery processes from the post-SMS decomposition product were thoroughly investigated. Optimal leaching conditions using 10 wt% HCl enabled efficient dissolution and

recovery of zirconium, achieving a leaching and recovery efficiency exceeding 98%.

4. An effective purification process for the zirconium precursor was developed through selective precipitation (via zirconium basic sulfate, ZBS), phase conversion, and hydrolysis. The zirconium recovery efficiency at the ZBS precipitation stage exceeded 99.3%, and following the complete purification and calcination sequence, the final ZrO_2 product achieved a purity of 99.57%.

5. Based on the experimental findings, an integrated technological chain for the deep processing of Vietnamese zircon concentrate—spanning KOH-SMS decomposition, acid leaching, silica removal, and intermediate purification to the preparation of high-purity ZrO_2—was successfully established. This technological chain achieves both high decomposition yield and high product purity, providing a robust scientific and experimental basis for the industrial deep processing of Vietnamese zircon concentrate.

6. Purified $ZrOCl_2$ obtained from the processing of Vietnamese zircon concentrate was successfully utilized as a precursor to synthesize an Mg–Zrcomposite catalyst. Preliminary catalytic evaluation demonstrated that the MgO–ZrO_2 material effectively catalyzes the conversion of lipid feedstocks (including high-free-fatty-acid oils and refined coconut oil) into biodiesel, achieving a fatty acid ethyl ester (FAEE) content exceeding 94%.